

Conductance of Finite-Scale Systems with Multiple Percolation Channels

E.Z. Meilikhov*

RRC “Kurchatov Institute”, 123182 Moscow, Russia

We investigate properties of two-dimensional finite-scale percolation systems whose size along the current flow is smaller than the perpendicular size. Successive thresholds of appearing multiple percolation channels in such systems have been determined and dependencies of the conductance on their size and percolation parameter p have been calculated. Various experimental examples show that the finite-scale percolation system is the natural mathematical model suitable for the qualitative and quantitative description of different physical systems.

PACS numbers: 64.60.Ak, 61.43.Bn, 72.80.Ng, 52.80.Mg

1. Introduction

The percolation threshold $p_{c\infty}$ for the *infinite* percolation system is the quite definite value depending on the system topology and dimension. When the percolation parameter p defining the fraction of conducting regions becomes higher, the *infinite* conducting cluster arises whose conductance is the smooth function of p [1]. Recently, the new remarkable results have been obtained for infinite rectangular lattices at critical value of p . Firstly, it has been found numerically that the probability of appearing the spanning cluster is an universal function the rectangular ratio only [2]. Secondly, it has been proved that more than one spanning cluster could exist in two-dimensional critical percolation systems [3], and, third, it has been shown by numerical calculations that there could be more than one cluster spanning the short direction of a long strip [4]. The exact formulae (the crossing formulae) for the probability that a certain number of crossing clusters (channels) span a long strip has been derived in [5].

However, all cited results refer to *infinite* systems only (or to the finite systems with lattice cell approaching zero which are equivalent to the infinite system). For the *finite-scale* system, the situation changes: the percolation threshold p_c corresponds to the formation of the *finite-scale* crossing cluster that connects opposite sides of the system. The threshold p_c becomes to be random quantity taking different values for various realizations of the system [6, 7]. In that case, one could say about the probability to get one or another value of p_c only or about the distribution function $f(p_c)$ of percolation thresholds for an ensemble of systems of the certain topology and geometry. For the infinite system $f(p_c) = \delta(p_c - p_{c\infty})$; for the finite-scale system, the distribution function becomes broader and the average threshold value $\bar{p}_c = \int p_c f(p_c) dp_c$ shifts (in one or another direction) relative to $p_{c\infty}$.

Finite-scale percolation system is the natural mathematical model of various physical systems: 1) two-dimensional electron gas near the surface of semiconductor with spatial potential fluctuations due to a non-uniform distribution of impurities [8], 2) cluster metal film whose resistance changes in the course of the deposition [9, 10], 3) hydrogenated amorphous silicon with its unusual noise features [11, 12] and even lightning discharges [13] (see below). In the most cases, the p -value is determined by a certain physical parameter that could be controlled. For instance, in non-uniform semiconductor the p -value is determined by Fermi level whose position could be changed by means of the gate potential, in cluster film the p -value varies temporally

in the course of the film growth, in *a*-Si it is defined by the hydrogen content. Therefore, various features of above-mentioned physical phenomena could be described by investigating percolation peculiarities for the respective model systems.

2. Percolation in finite-scale systems

For the system of square form, the distribution function $f_{\square}(p_c)$ of thresholds is close to the Gaussian one¹ [15]. For the rectangular system characterized by the aspect ratio L/h (h is the system “height”, L is its “length”) the distribution function $f(p_c)$ remains to be near-Gaussian, however the position of its maximum and the width are significantly changed. If the distribution function $f_{\square}(p_c)$ of thresholds for the square ($L/h = 1$) is known, then the distribution function for the system with $L \gg h$ could be found by means of the approximate relation

$$f(p_c) \approx (L/h)f_{\square}(p_c) \left[1 - \int_0^{p_c} f_{\square}(p_c) dp_c \right]^{L/h-1}. \quad (1)$$

Keeping in mind to study the conductance of percolation lattices similar to the long strip ($L \gg h$) and to use parameters of the relevant functions $f(p_c)$ for the description of conductance features (mostly, for the current flowing along h), we have performed numerical investigating the site percolation problem for the system comprising the finite-scale rectangular lattice with square cells. The ratio of the lattice height h and length L (being measured by the numbers of cells contained, respectively, along and transverse to the mean direction of the current flow through the lattice) has been varied in the broad enough range to study the percolation not only in the lattice of the square form but also along ($L/h \ll 1$) and across ($L/h \gg 1$) the narrow $h \times L$ -“strip”. Early, similar calculations (but for square systems of rather large sizes, $h = L > 32$, only and in the immediate vicinity of p_c) have been performed in [16, 17]. The percolation probability for rectangular systems of different aspect ratios for fixed p -values has been calculated in [18].

Results of percolation calculations for the site problem are presented in Figs. 1, 2 and lead to the following conclusions:

- the mean percolation threshold \bar{p}_c for the *square* lattice is close to the percolation threshold $p_{c\infty}$ of the infinite lattice (in our case, $p_{c\infty} \approx 0.59$);
- the mean percolation threshold *across* the narrow “strip” is significantly *lower* than $p_{c\infty}$;
- the mean percolation threshold *along* the narrow “strip” is *higher* than $p_{c\infty}$, with $\bar{p}_c \rightarrow 1$ at $L/h \rightarrow 0$;
- distribution functions of percolation thresholds are close to the Gaussian function $f(p_c) \propto \exp[-(p_c - \bar{p}_c)^2/2\sigma^2]$;
- the width σ of the distribution function $f(p_c)$ (defined by double standard deviation 2σ) is maximum for the square lattice;

¹More accurate calculations show the distribution function is slightly asymmetric and is not Gaussian (see Fig. 1). Moreover, its distinction from Gaussian function does not disappear even with increasing the lattice size [14].

- approximate formulae (1) leads to the correct (with accuracy better than 10%) parameter values of approximating Gaussian function².

In addition to the significant spread of percolations thresholds, another feature of the finite-scale percolation system is the possibility of the simultaneous existence of several clusters connecting its opposite sides and representing separate percolation paths [3, 20]. Here, the system conductance $G(p)$ ceases to be the smooth function of p and increases (with p) by more or less pronounced jumps corresponding to appearing new percolation paths. It is illustrated by Fig. 3 where the calculated dependence $G(p)$ for the transverse conductance of the long 10×1000 -strip on the p -value is shown (naturally, that is the result relative to one of numerous random realizations of such a system). The relevant numerical calculations for the site problem have been performed with applying the known transfer matrix method [21] for the lattice where the conductance of bonds between occupied sites (which fraction equals p) has been assumed to be $G_0 = 1 \text{ Ohm}^{-1}$, and conductances of all other bonds – to be $G_{\min} = 10^{-5}G_0$. Each jump of the conductance is on the order of value equal to $0.1 \text{ Ohm}^{-1} = G_0/10$. In consideration of $h = 10$, it means that successively appeared new conducting channels are isolated from each other and almost linear.

Considering the dependence $G(L)$ at a given p -value one could recognize how many percolation paths (parallel conducting channels) exist in the long strip $L \times h$ and how far are they from each other at that p -value. Indeed, the every sharp increase of the conductance $G(L)$ is the sign of appearing the new percolation channel. Let such jumps happen at the values L_i ($i=1, 2, \dots$). Then the difference $L_{i+1} - L_i$ is the distance between $(i+1)$ -th and i -th channels. It is just this dependence $G(L)$ which is determined naturally in the course of the conductance calculations by transfer matrix method. Several such dependencies (corresponding to the same random realization of 10×1000 -system as for Fig. 2) are displayed in Fig. 4. They show that the first conducting channel arises at $p \approx 0.3$, and already at $p \approx 0.45$ the number of such channels come up to ten, with their distribution over the system length being more or less uniform. However, even at $p \approx 0.5 < p_{c\infty}$ those channels merge and the current through the strip flows uniformly.

Percolation paths originating with increasing p could be of two kinds: they are either connected with the “old” paths (having aroused at lower values of the parameter p) or isolated completely from those, and then one could say about arising new percolation channel. The highest conductance jumps could be naturally associated with the percolation paths of the second type. Therewith, one could say about the successive (as p becomes higher) “switching” *different* percolation channels in the system. Obviously, that scenario is mostly probable in the systems whose width h (measured along the direction of the current flow) is much less than the length L . In what follows, we shall consider just that system and search the most probable values of the successive “percolation thresholds” $p_c^{(n)}$ corresponding to originating new percolation channels.

If the distribution function $f(p_c)$ for percolation thresholds (with the standard meaning of this term relating to originating the first percolation path) is known for a given system (for instance, by numerical modeling, see Fig. 1), then the sequence $\bar{p}_c^{(n)}$ ($n = 1, 2, \dots$) of the mean values of percolation thresholds could be found in the following way. The probability of falling

²It is the consequence of the known fact that transverse and longitudinal sizes of the cluster arising at the percolation threshold are nearly the same (about of h) [19])

the next (n -th) threshold within the interval from $p_c^{(n)}$ to $p_c^{(n)} + dp_c$ equals

$$f[p_c^{(n)}]dp_c = w[p_c^{(n)} > p_c^{(n-1)}] \cdot g_n[p_c^{(n)}]dp_c, \quad (2)$$

where $g_n[p_c^{(n)}]$ is the distribution function for n -th percolation threshold, and the probability that the n -th threshold has occurred after the $(n-1)$ -th threshold is equal to

$$w[p_c^{(n)} > p_c^{(n-1)}] = 1 - F[p_c^{(n-1)}], \quad F(t) = \int_0^t f(p_c)dp_c. \quad (3)$$

It follows herefrom

$$g_n[p_c^{(n)}] = \begin{cases} 0, & p_c^{(n)} < p_c^{(n-1)} \\ \frac{f[p_c^{(n)}]}{1 - F[p_c^{(n-1)}]}, & p_c^{(n)} > p_c^{(n-1)} \end{cases}. \quad (4)$$

To calculate the mean value $\bar{p}_c^{(n)}$ of the n -th threshold one has to perform n averaging procedures with the help of functions $g_k[p_c^{(k)}]$ ($k = n, n-1, \dots, 1$):

$$\langle p_c^{(n)} \rangle = \int_{p_c^{(n-1)}}^1 p_c^{(n)} g_n[p_c^{(n)}] dp_c^{(n)} = \frac{\Psi_1[p_c^{(n-1)}]}{1 - F[p_c^{(n-1)}]}, \quad \text{where} \quad \Psi_1(t) = \int_t^1 x f(x) dx,$$

$$\langle \langle p_c^{(n)} \rangle \rangle = \int_{p_c^{(n-2)}}^1 \langle p_c^{(n)} \rangle g_{n-1}[p_c^{(n-1)}] dp_c^{(n-1)} = \frac{\Psi_2[p_c^{(n-2)}]}{1 - F[p_c^{(n-2)}]}, \quad \text{where} \quad \Psi_2(t) = \int_t^1 \frac{f(x)\Psi_1(x)}{1 - F(x)} dx,$$

.....

$$\underbrace{\langle \dots \langle p_c^{(n)} \rangle \dots \rangle}_{k\text{-th averaging}} = \int_{p_c^{(n-k)}}^1 \underbrace{\langle \dots \langle p_c^{(n)} \rangle \dots \rangle}_{(k-1)\text{-th averaging}} g_{n+1-k}[p_c^{(n+1-k)}] dp_c^{(n+1-k)} = \frac{\Psi_{n-k}[p_c^{(n-k)}]}{1 - F[p_c^{(n-k)}]},$$

$$\text{where} \quad \Psi_{n-k}(t) = \int_t^1 \frac{f(x)\Psi_{n-1-k}(x)}{1 - F(x)} dx,$$

.....

$$\bar{p}_c^{(n)} \equiv \underbrace{\langle \dots \langle p_c^{(n)} \rangle \dots \rangle}_{n\text{-th averaging}} = \Psi_n(0), \quad \text{where} \quad \Psi_n(0) = \int_0^1 \frac{f(x)\Psi_{n-1}(x)}{1 - F(x)} dx.$$

With those recurrent relations one could calculate successively all mean values $\bar{p}_c^{(n)}$.

It is difficult to perform analytically this procedure for the above-found distribution $f(p_c)$, which is close to the Gaussian one. However, with that distribution taken approximately as the uniform distribution

$$f(p_c) = \begin{cases} \frac{1}{4\sigma}, & |p_c - \bar{p}_c| < 2\sigma \\ 0, & |p_c - \bar{p}_c| > 2\sigma \end{cases} \quad (5)$$

of the width 4σ centered near $p_c = \bar{p}$, the mentioned procedure yields the simple result

$$\bar{p}_c^{(1)} = \bar{p}_c, \quad \bar{p}_c^{(n)} = \bar{p}_c + 2\sigma \left(1 - \frac{1}{2^{n-1}} \right), \quad (6)$$

according to which the mean value of each threshold lies exactly in the middle between the preceding threshold and the value of $p_c = \bar{p}_c + 2\sigma$ corresponding to the right boundary of the adopted uniform distribution.

In the insert of Fig. 3, the values of successive thresholds $\bar{p}_c^{(n)}$ ($n = 1, \dots, 6$) are shown for the typical 10×1000 -lattice. With increasing n -number, thresholds converges rapidly and their values are well approximated by the Eq. (6).

3. Experimental examples

In this section, we consider some physical phenomena that are different in all respects excluding the only one: their properties could be described in the framework of simple percolation models exploiting the above-derived results.

Cluster films. Conducting cluster films are produced by the generation and the subsequent deposition of small (diameter of 10–100 nm) metal clusters on the insulator substrate with preliminary deposited contacts. At a certain film thickness (increasing in the course of the film deposition), the gap between the contacts becomes conducting. In the experiments [9, 10], Bi-clusters of the size 60 ± 10 nm have been deposited on the SiN-substrate. In the course of the deposition, the current I between metal contacts separated by the distance of $h \sim 1000$ nm has been measured, with the contact width of $L \gg h$ and the voltage drop of ~ 1 V.

One of the temporal dependencies $I(t)$ of the current (given in [9]) is displayed in Fig. 5. In the course of the deposition, the fraction p of the surface occupied by the clusters increases gradually and at one point the current rises steeply (on three orders of value) that corresponds to originating the first percolation channel, whereupon the current increases by well-marked steps of lesser heights corresponding to appearing the next percolation channels, and finely approaches to saturation. The insert of Fig. 5 shows the typical result of modeling that process by calculating the conductance dependence $G(p)$ for one of the realizations of the 10×50 -lattice (the site problem for the lattice with square cells has been solved); to fit the relative value of the main conductance jump, the value $G_{\min}/G_0 = 10^{-7}$ has been chosen. The clear resemblance of the experimental and the model dependencies is indicative of adequacy of our model for describing the process of the film growth and the possibility to calculate qualitatively characteristics of that process³.

Another interesting and important feature of conducting cluster films (having observed after the deposition completion) is the current noise indicating of spontaneous temporal alterations of the film conductance. Fig. 6 shows the typical temporal dependence $I(t)$ of the current flowing through the cluster film that demonstrates the occurrence of the intensive random noise of the “telegraph” type [10] against the smooth background of the conductance change due to the film oxidation (shown by the dash curve). The relative current variations are of about 10%. In the insert of Fig. 6, the typical result of modeling that process is shown. Conductance variations $G(t^*)$ for one of the realizations of the 10×50 -lattice system with $p = 0.25$ have been monitored in the course of commutating status of randomly chosen sites: the existent site has

³Some more elaborated model of the film deposition is considered in [22]. However, the system of the square form where appearing the parallel percolation channels is improbable has been studied only.

been removed, while the absent one has been recovered. The flow of “time” t^* corresponds to the sequence of those commutations. Like in the experiment, the relative conductance variation equals $\sim 10\%$. The occurrence of the “telegraph” noise in the considered percolation system is associated with the disparity of their sites: some of them are included in the skeleton cluster determining the average system conductance or close to its sites, while other sites are apart from them. Therefore, “switching on” or “switching out” the sites of the first type changes significantly the system conductance (in our case, on the order of $\sim 10\%$), while the status of the second type sites influences the conductance slightly. It is seen from Fig. 6 that the stepwise variation of the conductance occur on rare occasions – only one attempt among ~ 100 is “successful”. It means that in the considered system the current-conducting cluster includes $\sim 1\%$ of all sites only.

The insert of Fig. 6 demonstrates also the model temporal dependence $G(t^*)$ of the conductance for one of the realizations of the 10×50 -lattice system with $p = 0.85$. In that case, there is no telegraph noise, and the relative conductance fluctuations are significantly less than 10% . That agree with experimental results corresponding to the virgin (non-oxidized) cluster films with higher p -value [10] or – to observations of the noise in amorphous a -Si-films [11, 12].

Two-dimensional electron gas in the system with random electrostatic potential.

The structure “metal-insulator-semiconductor” is the standard tool for controllable producing two-dimensional electron gas (near the interface insulator-semiconductor). Built in such a structure electric charges (localized in traps of the gate insulator, for instance) produce a random electrostatic potential in the region of two-dimensional electron channel. As this takes place, electrons are localized in wells of chaotic potential relief and the system turns into percolation one. The current in such a system flows through “bonds” that connect potential wells - “sites” and transit mountain crossings (saddle-points) of the potential relief.

At low electron Fermi energy ε_F , those crossings (relative to the Fermi level) are of high-altitude and, hence, the conductance is of the activation nature and low. With rising the Fermi level (being controlled by the gate potential V_g), crossing heights diminish and they gradually “drop out”⁴. In that regime, the conductance is of the percolation nature and rising the Fermi energy is equivalent to variation of the percolation parameter p related to the number of “weak links” – former crossings of the potential relief.

The percolation parameter p could be associated with the relative fraction of that part of the system surface where $V < \varepsilon_F$, so

$$p = \int_{-\infty}^{\varepsilon_F} \phi(V) dV.$$

Near the percolation threshold $\Delta p \propto \Delta \varepsilon_F$ and, besides, $\partial \varepsilon_F / \partial V_g = \text{Const}$ [8]. Therefore, the gate voltage V_g and the percolation parameter p are connected by the linear relationship $\Delta V_g \propto \Delta p$ permitting the simple comparison of experimental dependencies $G(V_g)$ with calculated relations $G(p)$ (see below).

In experiments [8], there have been two-dimensional electron channel with $h = 5 \mu\text{m}$, $L = 50 \mu\text{m}$ and the characteristic size of percolation cluster cells of about $1 \mu\text{m}$ that corresponds

⁴At some value of the Fermi energy, the total conductance of the system is defined by the “weak link” conductance G_q corresponding to the highest saddle-point on the current path [8]. Electron flow through this saddle-point is quasi one-dimensional that (at low enough temperatures) leads to the quantization of the conductance $G_q = (e^2/\pi\hbar)N$ ($N = 1, 2, \dots$) [23]. The present paper does not touch on this interesting effect.

approximately to the percolation 10×100 -lattice. Fig. 7 compares the experimental dependence $G(V_g)$ with the dependence $G(p)$ calculated by the above-described method (values $G_0 = 2.5 \cdot 10^{-4} \text{ Ohm}^{-1}$, and $G_{\min} \ll G_0$ have been accepted). It is seen that both dependencies are well superimposed⁵ at $p \gtrsim 0.3$ with the preservation of the linear relationship between V_g and p . That argues in favor of the above-suggested assumption about the percolation nature of the examined system at high values V_g . At lower V_g -values the conductance is the activation one and its description requires modifying the simple considered model.

Lightning. The lightning is the mighty short-time electric discharge in the atmosphere whose length is usually measured by kilometers. Lightning discharge is always preceded by the leader pre-discharge which appears at the electric field intensity as low as $\sim 3 \text{ kV/cm}$ that is on the order of magnitude lower than the electric field necessary for the electric breakdown in air at normal conditions (30 kV/cm). Various lightning theories overcome that discrepancy by rather artificial assumptions. Another unusual feature of the leader is that its travel to the earth occurs by steps separated by pauses, so that it has been referred as the stepped leader. In recent years, there has been suggested the new hypothesis [13] of initiating lightnings (producing leaders) by cosmic rays of ultra-high energies (higher than 10^{12} eV). Charged particles born by the rays (electrons, muons) pass through the atmosphere and leave behind the system of ionized traces of different length and various directions – a kind of a random *permanently renewed* lattice of conducting bonds, along which first the leader goes forward and then occurs the lightning discharge.

Estimates [13] show that the typical size of the lattice cell is of about 100 m. With the distance from the bottom surface of the thunder cloud to the earth of $0.5 - 3 \text{ km}$ and its length of $10 - 30 \text{ km}$, that corresponds to the percolation lattice $h \times L = 10 \times (100 - 500)$

The problem concerning the value of the percolation parameter p involves the special examination. If the system would be stationary, the rough estimate of p could be obtained on the base of the following consideration. In addition to single lightning discharges, simultaneous multiple discharges are frequently observed which could be associated with multiple percolation channels of above-considered model. To estimate the average number of lightning channels $\langle N \rangle$ for those multiple discharges we have studied numerous lightning pictures published in Internet (the total number of about 350; see, for instance, [24]) and derived $\langle N \rangle = 3 \pm 1$. On the other hand, that number is determined by dimensions of the percolation $h \times L$ -lattice and the percolation parameter p . Investigating dependensies similar to those shown in Fig. 4 (but relating to different realizations of 10×300 -lattices) leads to $\langle N \rangle \approx 3$ if one accepts $p = 0.3 - 0.4$.

However, proceeding from the known intensity of cosmic rays one could conclude that the obtained estimation is too high: the fluence of cosmic rays with the needed energy is sufficient for producing (in the moment) the system of ionized traces with $p \sim 0.01$. According to Fig. 1, the probability of generating conducting channel in that system is negligible, i.e., the lightning would be absolutely unique phenomenon. Nature overcomes that difficulty executing the breakdown of the air gap between the cloud and earth by means of the *stepped* leader discharge. Each successive step of its expansion occurs after the pause during which the leader waits for generating (by cosmic rays) a new ionized trace allowing to go forward. In the context of the percolation theory, there arises the new problem concerning the delayed, or stepped,

⁵The existence of steps on the calculated curve is the consequence of simplifying assumption that conductances of all bonds are equal. In the real experiment, the spread of those conductances results in smoothing peculiarities on the $G(V_g)$ -curve.

percolation in the *time-dependent* lattice of bonds.

4. Conclusions

March to new technologies allowing the successive diminishing characteristic dimensions of electronic devices transforms the latter into mesoscopic systems whose properties are identical on the average only. Many of them are intrinsically finite-scale percolation systems whose characteristic dimensions exceed the size of constituent elements by 10–100 times (and on occasion – by several times only). In the present paper, some features of such two-dimensional systems have been studied. In particular, there have been investigated statistical properties of their percolation thresholds, defined successive thresholds of arising multiple percolation channels, calculated the conductance dependence of such systems on their dimensions and percolation parameter p . Special attention has been given to systems whose dimension along the direction of the current flow is significantly smaller than in the direction perpendicular to the current. It has been shown that percolation finite-scale systems are natural mathematical models suitable for the qualitative and quantitative description of different physical systems.

This work was supported by Grants 03-02-17029, 05-02-17021 of the Russian Foundation of Basic Researches.

Figure captions

Fig. 1. Distribution function $f(p_c)$ of percolation thresholds (site problem) for random rectangular lattices with square cells defined with numerical calculations of thresholds for 10^5 realizations of each system (threshold for the infinite lattice is $p_{c\infty} \approx 0.59$). Marking of distributions corresponds to lattice dimensions in the format $h \times L$. Curves are approximations of distribution functions by Gaussian ones.

Fig. 2. Parameters of Gaussian functions approximating the distribution functions $f(p_c)$ of percolation thresholds for random lattices of different dimensions shown in Fig. 1. Three top curves – mean threshold values \bar{p}_c , three bottom curves – widths of distributions σ .

Fig. 3. Typical dependence $G(p)$ of the transversal conductance of a random 10×1000 -lattice in the form of the long strip on the p -value. Arrows indicate specific p -values (successive percolation thresholds $p_c^{(n)}$) corresponding to originating new conducting channels. In the insert – $p_c^{(n)}$ -values corresponding to the dependence $G(p)$ shown (\bullet) and the analytical relation (6) (\circ).

Fig. 4. Dependence $G(L)$ of the transversal conductance of a typical random lattice of increasing length with $h = 10$ and $1 < L \leq 1000$ on its length L at $p = \text{Const}$. Each jump corresponds to linking up the section containing the conducting channel.

Fig. 5. Temporal dependence of the current $I(t)$ through the cluster film in the course of its deposition [9]. In the insert – dependence of the 10×50 -lattice conductance $G(p)$ with the ratio $G_{\min}/G_0 = 10^{-7}$.

Fig. 6. Temporal dependence of the current $I(t)$ through the cluster film after terminating the process of its deposition (the voltage equals 5 mV, $T = 300$ K) [10]. In the insert – “temporal” dependences $G(t^*)$ of 10×50 -lattice conductance for $p = 0.25$ and $p = 0.85$.

Fig. 7. Experimental conductance dependence $G(V_g)$ for two-dimensional electron gas in the electrostatically disordered structure “metal-insulator-semiconductor” ($T = 300$ K) on the gate voltage [8] (dotted curve; bottom and left coordination axes) and the typical calculated conductance dependence $G(p)$ for the percolation 10×100 -lattice (bond problem) on the percolation parameter p (dots; top and right coordination axes).

*Electronic address: meilikhov@imp.kiae.ru

References

- [1] D. Stauffer, A. Aharony, *Introduction to Percolation Theory* (Taylor& Francis, London, 1994).
- [2] R. Langlands, C. Pichet, P. Pouliot, and Y. Saint-Aubin, *Stat. Phys.*, **67**, 553 (1992).
- [3] M. Aisenman, *Nucl. Phys. B*, **485**, 551 (1997).
- [4] C.-K. Hu, and C.-Y. Lin, *Phys. Rev. Lett.*, **77**, 8 (1996).
- [5] J. Cardy, *J. phys. A*, **31**, L105 (1998)
- [6] R. P. Langlands, C. Pichet, Ph. Pouliot, Y. Saint-Aubin, *J. Stat. Phys.*, **67**, 553 (1992).
- [7] J. H. Cardy, *J. Phys. A*, **25**, L201 (1992).
- [8] B. A. Aronzon, D. A. Bakaushin, A. S. Vedeneev, A. B. Davydov, E. Z. Meilikhov, and N. K. Chumakov, *Semiconductors*, **35**, 436 (2001).
- [9] J. Schmelzer, Jr., S. A. Brown, A. Wurl, M. Hyslop, R. J. Blaikie, *Phys. Rev. Lett.*, **88**, 226802 (2002).
- [10] M. Schulze, S. Gourley, S.A. Brown, A. Dunbar, J. Partridge, R. J. Blaikie, *Eur. Phys. J. D*, **24**, 291 (2003).
- [11] C. E. Parman, N. E. Israeloff, J. Kakalios, *Phys. Rev. B*, **47**, 12578 (1993).
- [12] L. M. Lust, J. Kakalios, *Phys. Rev. Lett.*, **75**, 2192 (1995).
- [13] V.I. Ermakov, Y.I. Stozhkov, *Proc. of 11th Int. Conf. on Atmospheric Electricity, Alabama, USA*, 242 (1999).
- [14] D. Stauffer, *Physica A*, **242**, 1 (1997).
- [15] B.I. Shklovskii, A.L. Efros, *Electronic properties of doped semiconductors* (Springer, Heidelberg, 1984).
- [16] C.-K. Hu, *Phys. Rev. B*, **51**, 3922 (1995).
- [17] C.-K. Hu, C.-Y. Lin, J.-A. Chen, *Phys. Rev. Lett.*, **75**, 193 (1995).
- [18] S. Tsubakihara, *Phys. Rev. E*, **62**, 8811 (2000).
- [19] R.A. Monetti, E.V. Albano, *Z. Phys. B*, **90**, 351 (1993).
- [20] C.-K. Hu, C.-Y. Lin, J.A. Chen, *Phys. Rev. Lett.*, **75**, 193 (1995).
- [21] B. Derrida, J. Vannimenus, *J. Phys. A*, **15**, L557 (1982).
- [22] N.I. Lebovka, S.S. Manna, S. Tarafdar, and N. Teslenko, *Phys. Rev. E*, **66**, 066134 (2002).

[23] M. Buttiker, Phys. Rev. B, **41**, R7906 (1990).

[24] <http://www.strikingimages.com/light.htm>

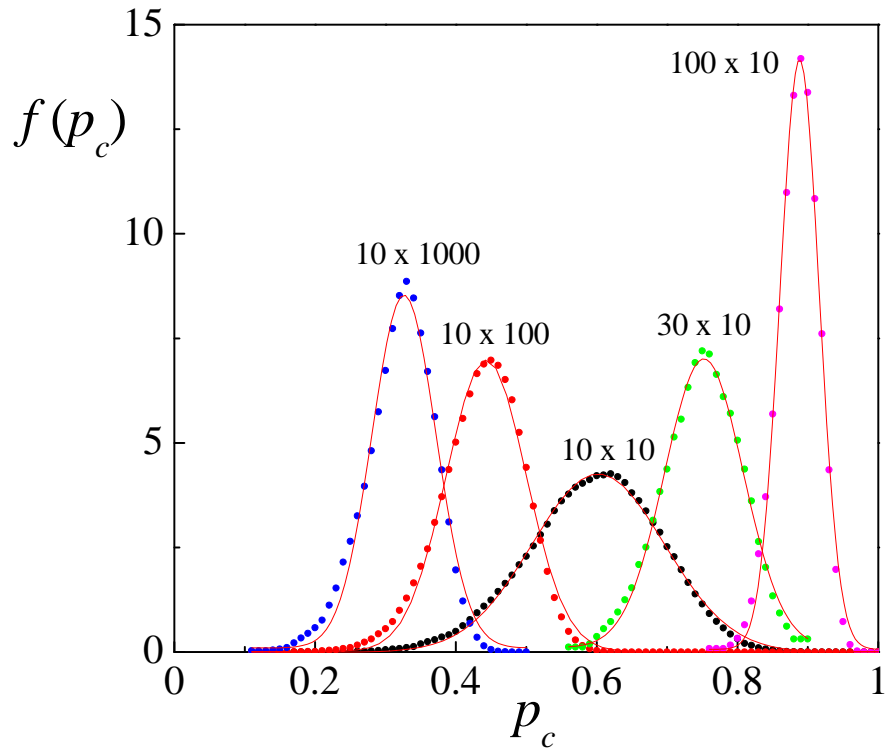


Fig. 1

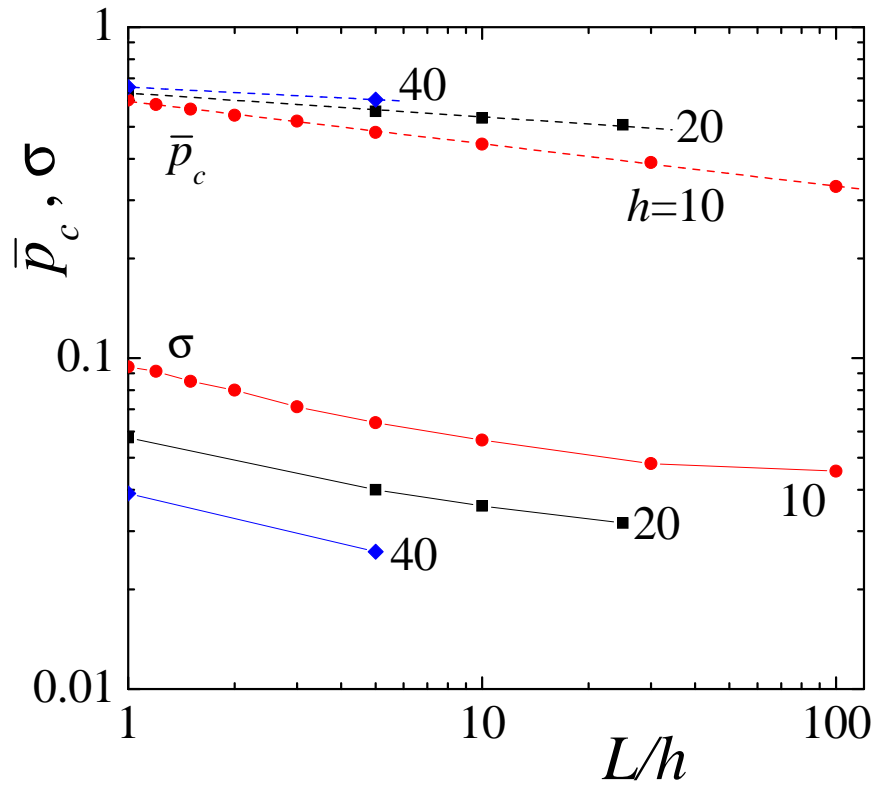


Fig. 2

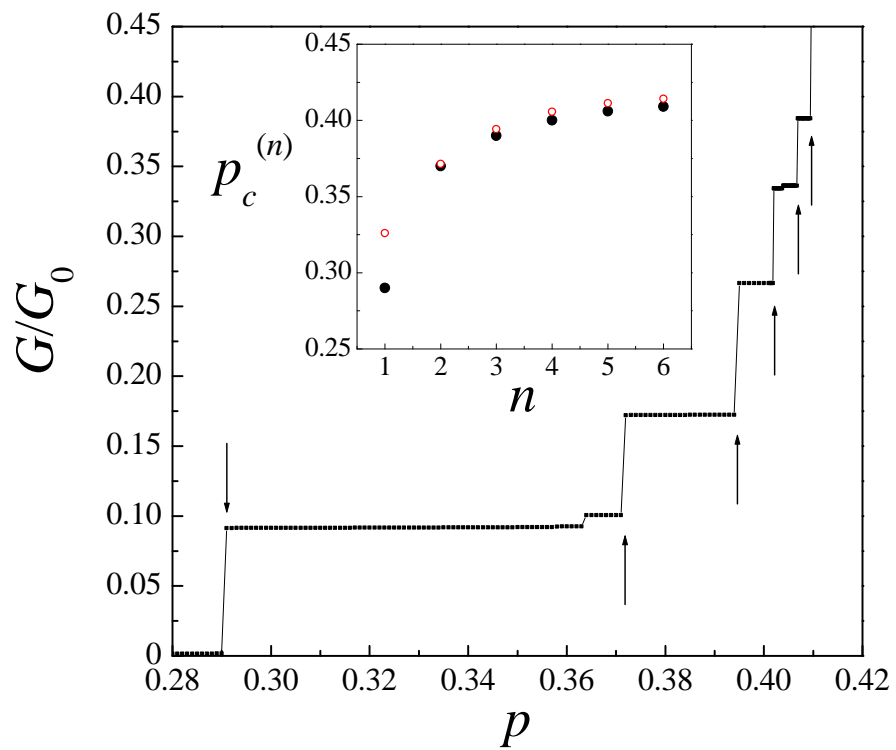


Fig. 3

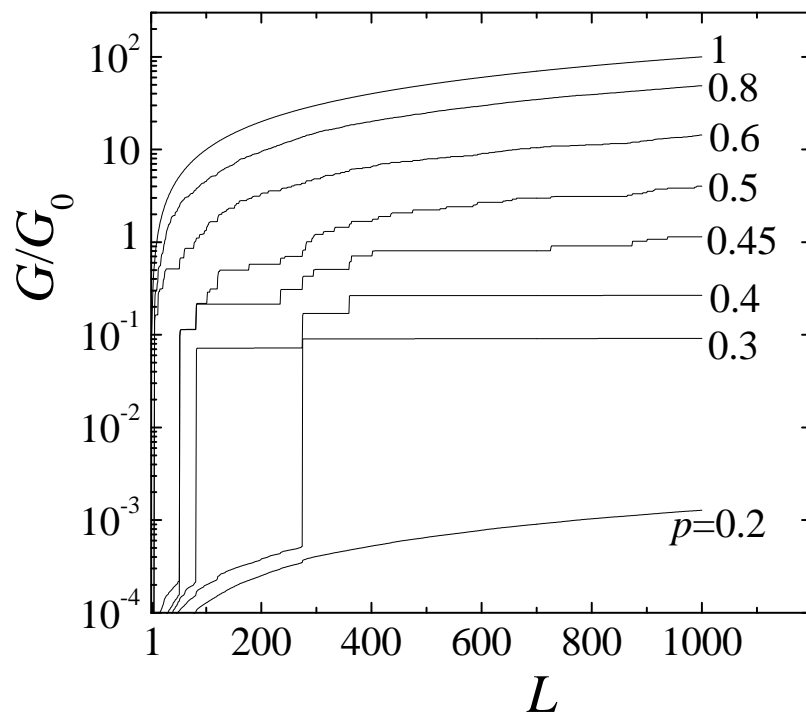


Fig. 4

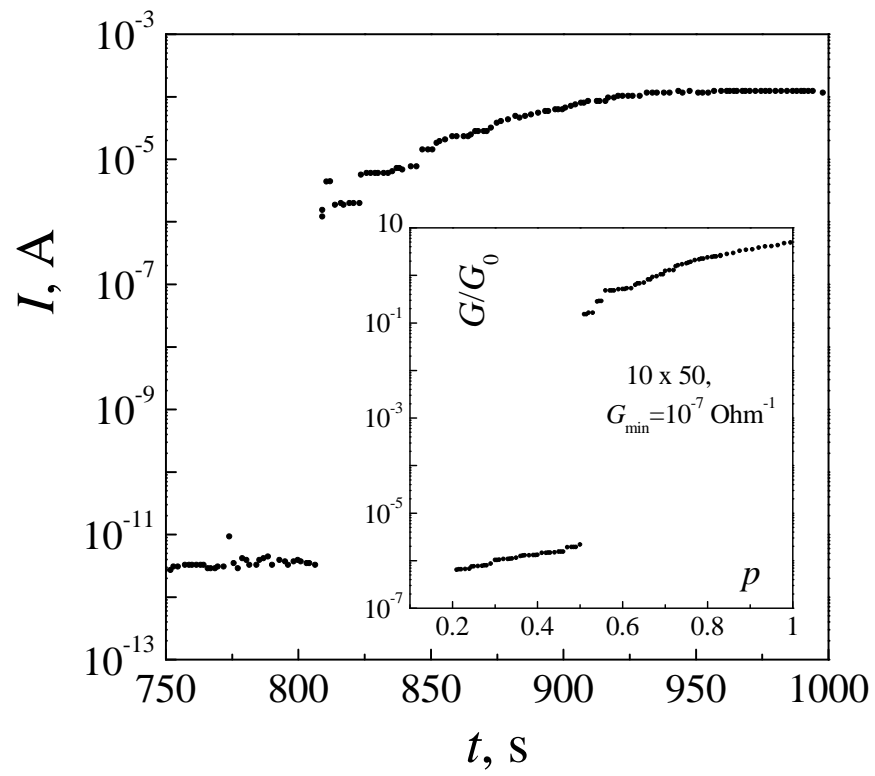


Fig. 5

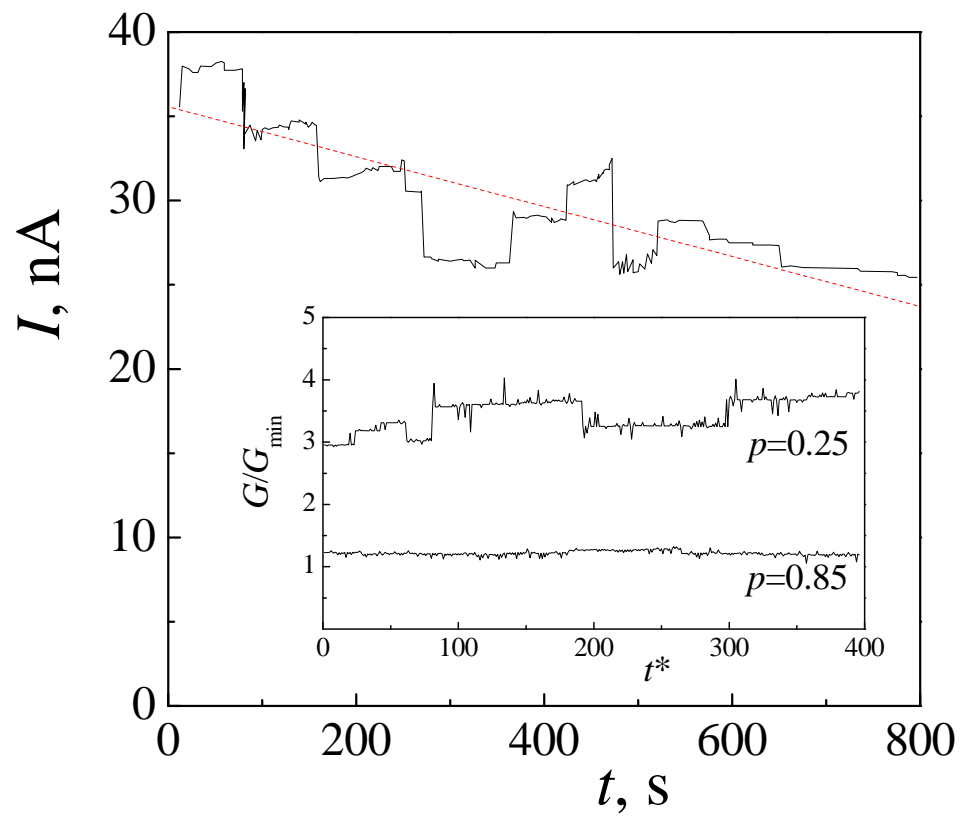


Fig. 6

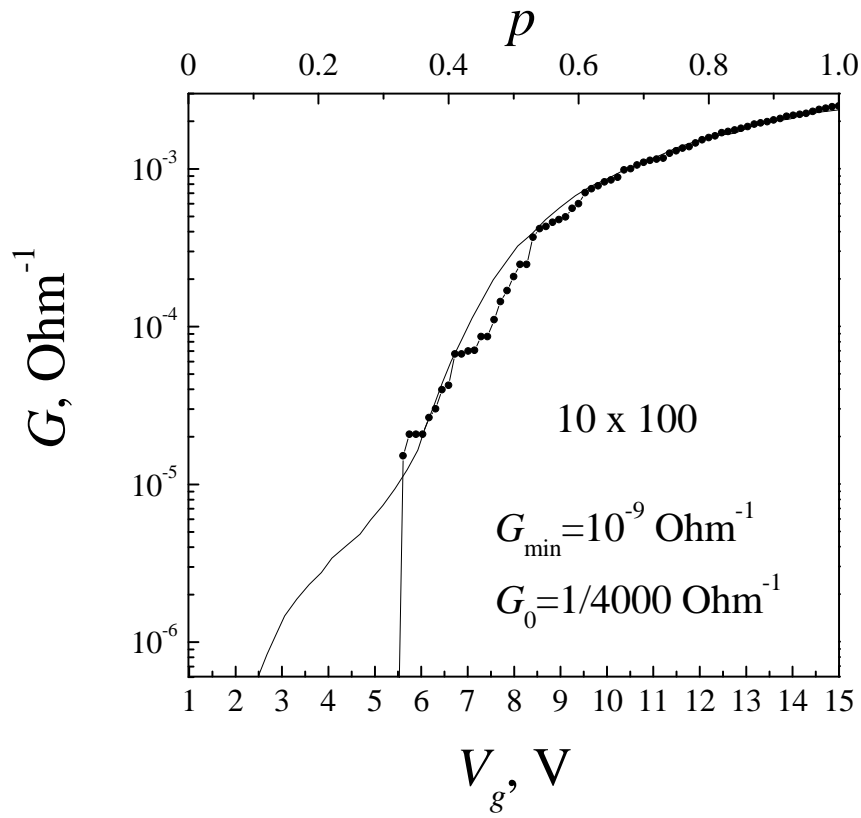


Fig. 7